Effect of indenter size on delamination initiation in glass fibre reinforced polymers (GFRP) under transverse loading

S. YUEN
Department of Mechanical Engineering, University of Alberta, Edmonton, AB, Canada, T6G 2G8

T. KUBOKI
Resin Systems Inc., Edmonton, AB, Canada T5M 3C5

P.-Y. B. JAR, T. W. FOREST
Department of Mechanical Engineering, University of Alberta, Edmonton, AB, Canada, T6G 2G8

J. J. R. CHENG
Department of Civil & Environmental Engg, University of Alberta, Edmonton, AB, Canada, T6G 2G7

Susceptibility to damage from concentrated transverse loading is one of the major weaknesses for many structures made of advanced fibre composites. Its importance has prompted development of standards [1, 2] to evaluate the resistance of fibre composites to such a loading mode. Using the set-up recommended in Ref. [1], we recently found that two mechanisms were responsible for the initiation of delamination under transverse loading. These are matrix shear cracking commencing around mid-thickness and contact indentation on the specimen surface [3]. The study showed that the test set-up generated contact indentation before the matrix shear cracking, but the latter initiated delamination first. Therefore, it was not clear whether the presence of surface indentation affected the critical load required for the development of delamination from the matrix shear cracking. As this information is essential for finite element modelling to obtain the criteria for delamination initiation and growth, a study was commenced to search for the set-up conditions that could suppress the surface indentation. It was soon discovered that an indenter with a spherical nose of sufficiently large diameter was able to suppress the surface indentation. In this work, indenters of different sizes were used to determine critical load for the on-set of delamination. Based on results obtained from the work, this paper discusses the effect of surface indentation on the critical load for delamination initiation.

The study used glass-fibre-reinforced polymers (GFRP), fabricated by a wet hand lay-up technique. Isophthalic polyester was used as the matrix (provided by Triple M Fibreglass Mfg. Ltd., Edmonton) and

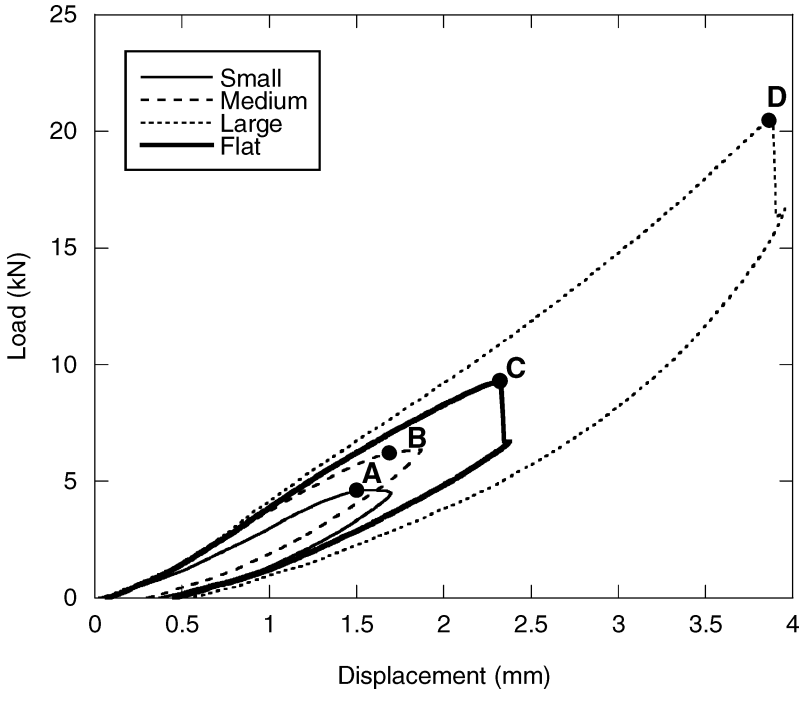

Figure 1 Typical load-displacement curves for the GFRP under transverse loading using different indenters. Points A, B, C and D represent the onset of delamination.

0022–2461

unidirectional glass fibre fabric of 9-oz/yd^2 for the reinforcement (provided by ZCL Composites, Edmonton). The unidirectional fibre fabric consisted of parallel fibre bundles stitched together at gaps of around 1 mm. Due to the presence of the gaps between the fibre bundles, resin-rich regions existed within each ply and between the plies of fibre reinforcement.

The fibre lay-up was $[(0/90)_6]_s$ and it generated a nominal thickness of 6.4 mm. Overall fibre volume fraction was around 45%, calculated using the following equation [4]:

$$\%V_f = \frac{\text{FAW} \times N \times 100}{\text{FD} \times 2h}$$

where FAW is area weight of the fibre fabric (9 oz/yd^2 or 0.3046 kg/m^2), N number of fibre layers (equal to 24 in this study), FD fibre density (2560 kg/m^3), and 2 h specimen thickness (0.0064 m). Each plate was machined to 4 specimens of 98 × 98 mm^2 for the transverse loading tests. At least 3 specimens were tested in each loading condition.

The transverse loading tests were conducted using Instron Universal Test Machine at a crosshead speed of 1.27 mm/min for both loading and unloading. The specimens were firmly clamped using a pneumatic clamp device, provided by Instron, which was designed based on the ASTM standard D3763-02 [1].

Four indenters were used in the study. In addition to the standard indenter with a spherical nose of 12.7 mm in diameter, two indenters with a spherical nose of 38.1 and 254 mm in diameter, respectively, and one cylindrical indenter of 12.7 mm in diameter with a flat end were used. The indenters with spherical noses are referred to

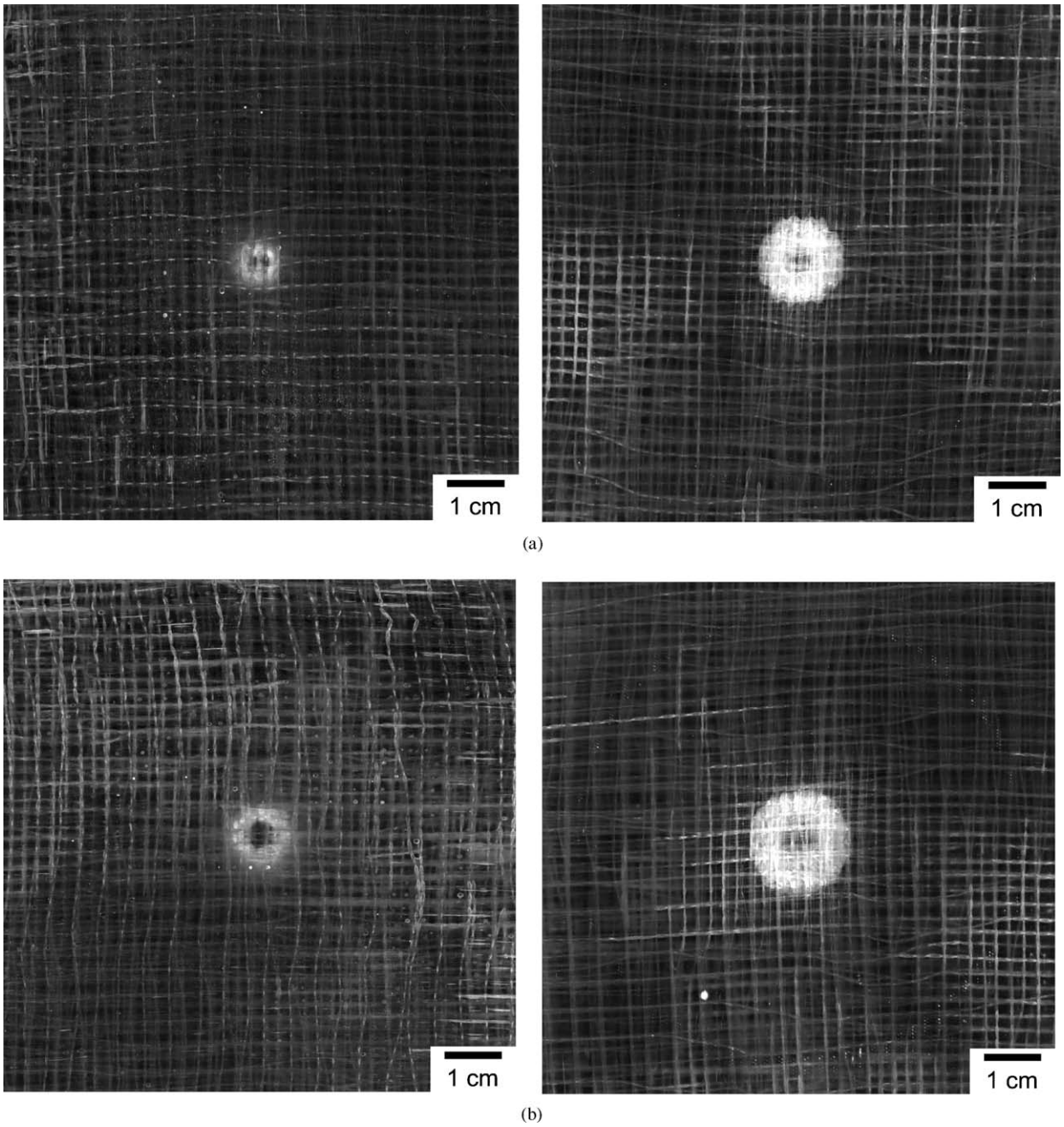

Figure 2 Images of the contact and back surfaces of specimens for Fig. 1: (a) small indenter, (b) medium indenter, (c) large indenter, and (d) flat indenter. Left image is the contact surface; right image is the back surface. (*Continued*)

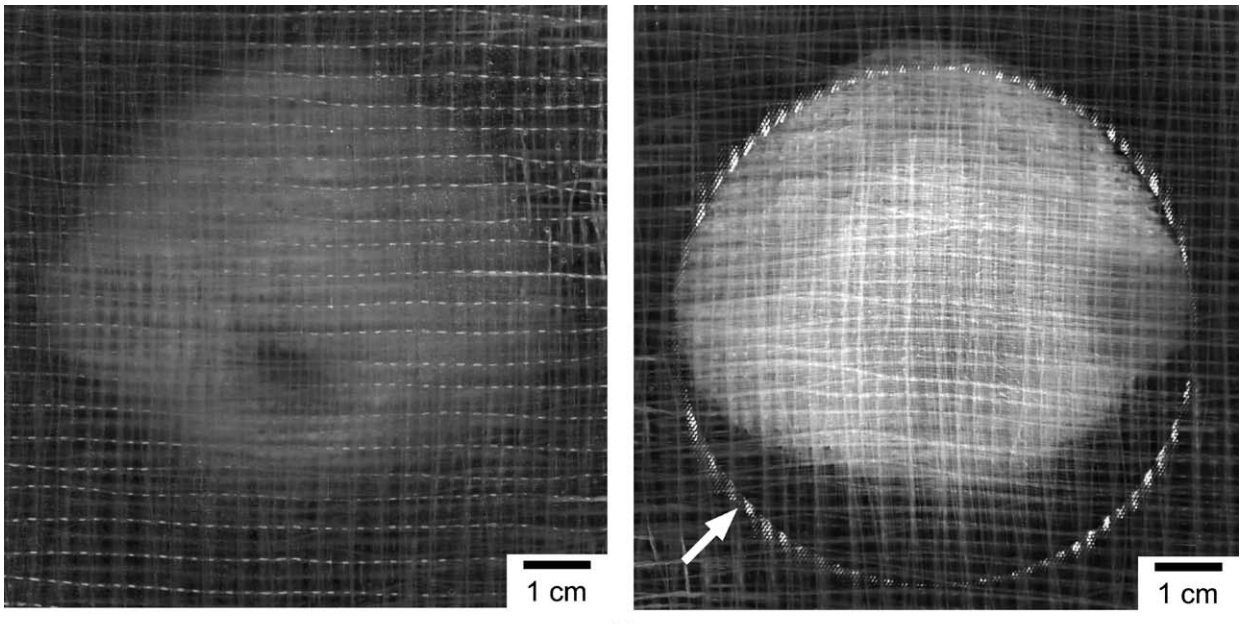

(c)

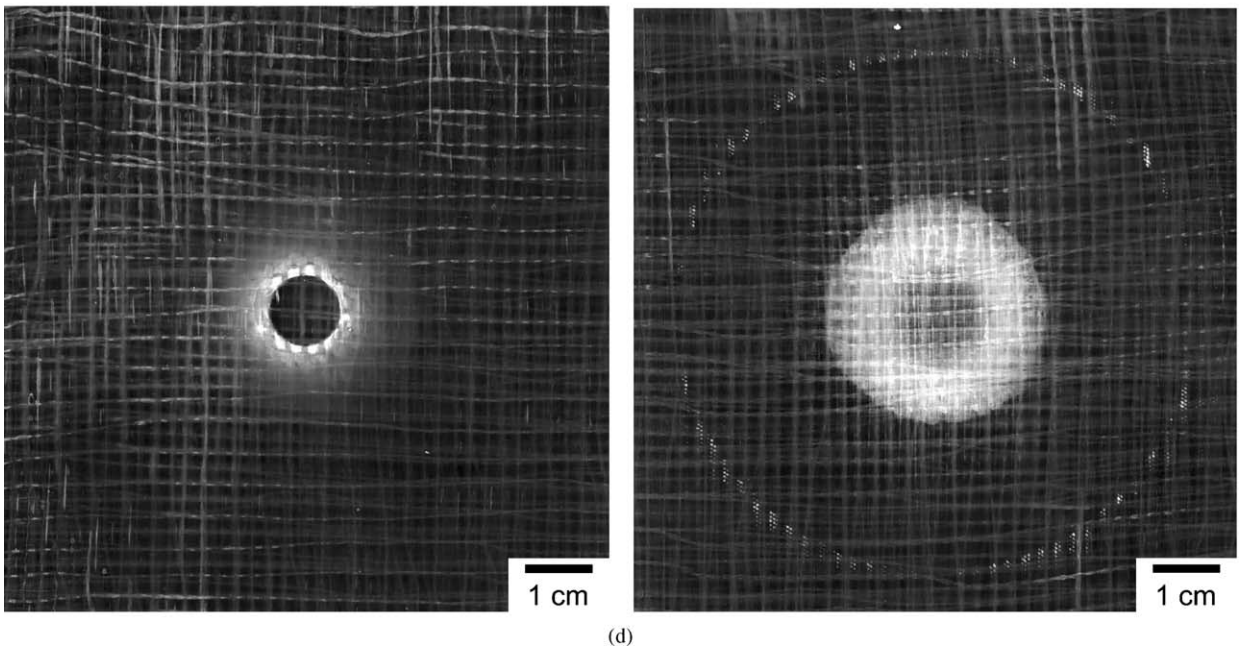

(d)

Figure 2 (*Continued*).

as small, medium and large indenters in the rest of the text, based on the size of the spherical nose. The flat indenter had its edge rounded with a radius of curvature of 1.27 mm, to reduce stress concentration generated by the contact circumference. Therefore, the true flat circular area at the end of the indenter had a diameter of 10.16 mm.

Displacement of the indenters was measured using a linear variable differential transformer (LVDT). The maximum contact area between the indenter and the GFRP specimen was recorded using a carbon paper placed between the specimen and the indenter. The recorded contact area was then scanned into a digital image; the contrast of the image was enhanced using an image processor (Adobe Photoshop 5.0.2).

Due to the translucent nature of the GFRP specimens, delamination damage could be seen from the specimen surface. Therefore, surfaces of the tested specimens were also scanned into digital images with contrast enhanced using the same image processing software.

Fig. 1 shows typical load-displacement curves using small, medium, large and flat indenters. All the curves show a monotonic increase of the load with displacement. The maximum load used for each indenter is equivalent to the load required for the on-set of delamination which corresponds to either a drastic change in slope at points A and B for the small and medium indenters, respectively [3, 5], or a sudden drop of the force, points C and D for the large and flat indenters, respectively. It should be noted that if the load was further increased from these points, no significant drop in load would have occurred until fibre fracture on the tensile side of the specimens. The curves clearly show that the load for the on-set of delamination was affected by the indenter size and geometry (spherical or flat). In addition, the figure suggests that unstable delamination

occurred by using the large or the flat indenter, possibly due to the high level of strain energy stored in the specimen before the on-set of delamination.

Fig. 2 shows the delamination damage viewed from the contact surface and the back surface. The images have been oriented in such a way that fibre in the surface layer is in the vertical direction. Some bending cracks, parallel to the fibre in the surface layer, can be seen on the back surfaces, which are mixed with bright square meshes that represent threads stitching the fibre bundles together. Delamination is clearly visible from the back surface, which appears to be much brighter than the surrounding area. For specimens loaded by the flat indenter, Fig. 3d, a distinctly bright circular ring of indentation damage can be seen on the contact surface, around the circumference of the contact area. The high loading level introduced by the flat and the large indenters also introduced a distinct bright circular ring on the back surface of the specimens, as indicated by a white arrow in Fig. 2c, which is the imprint of the circular hole (76.2 mm in diameter) in the clamping plate.

All the images from the back surfaces in Fig. 2 clearly show the delamination generated by the transverse loading. On the contact surfaces, the images suggest that the flat indenter introduced the most severe indentation damage, with possibility of fibre fracture, and the large indenter did not generate any indentation damage. Due to the translucent nature of the specimens, the delamination area is vaguely visible from the contact surfaces, appearing as a bright grey area.

The contact area between the indenter and the specimen at the maximum displacement is presented in Fig. 3. As expected, the size of the contact area varies, depending on the indenter used for the transverse loading. For the flat indenter, Fig. 3d, the contact size is very close to the diameter of the indenter, 10.16 mm.

Fig. 4 summarizes results from the transverse loading tests. The first plot, Fig. 4a, is the indentation force for delamination (from Fig. 1) versus diameter of the

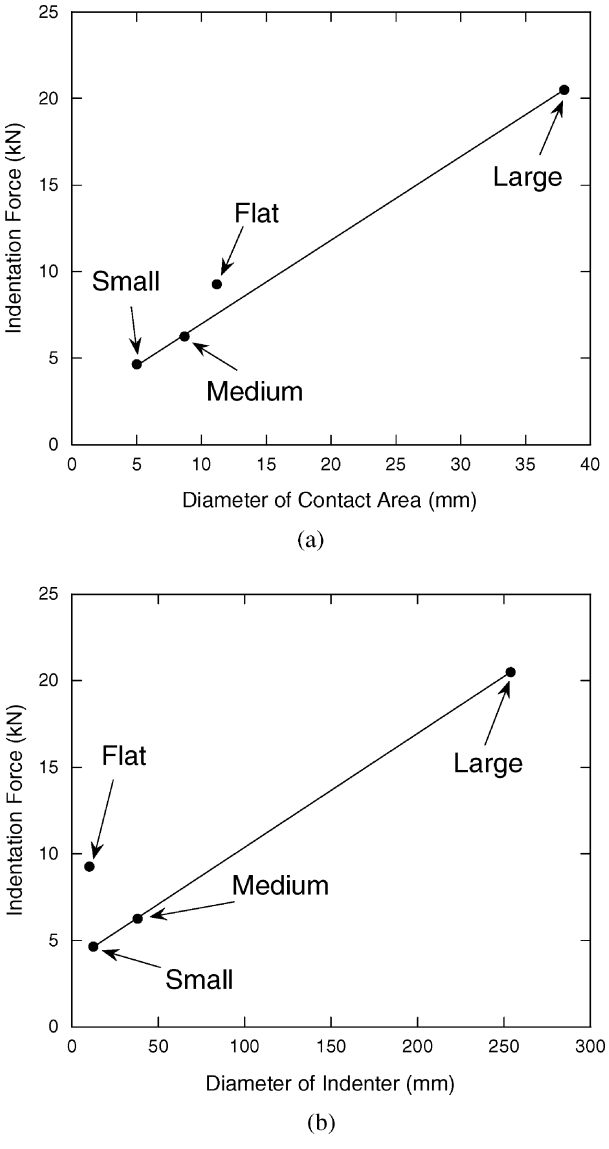

Figure 4 Plot of the indentation force for delamination versus: (a) diameter of the contact area, and (b) diameter of the indenter. The solid line in both figures is a least squares linear fit to data for the spherical indenters.

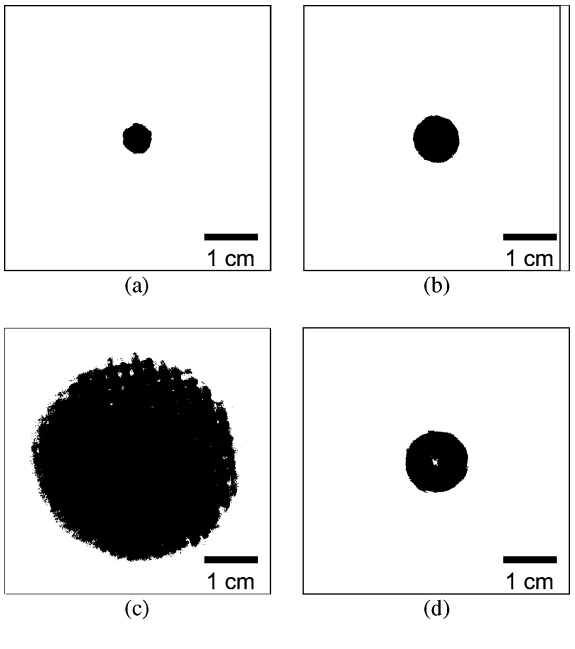

Figure 3 Images of contact area on the specimen surface: (a) small indenter, (b) medium indenter, (c) large indenter, and (d) flat indenter.

contact area (from Fig. 3). Results from the three spherical indenters fall on a straight line, despite the fact that specimens for the small and medium indenters contain indentation damage and those for the large indenter do not. The flat indenter, on the other hand, does not fall on this line. The same conclusion can be drawn from Fig. 4b, which is a plot of the indentation force for delamination versus diameter of the indenter. For the flat indenter, the diameter of the contact area is actually the size of the indenter used, which does not reflect the extent of indentation damage on the specimen surface. Thus, the results from the flat indenter do not fall on the straight line in Fig. 4. The results indicate that the force for delamination can be predicted when an indenter with a spherical nose is used for transverse loading. Prediction of the force does not require consideration of the indenter size, nor the corresponding indentation damage.

In conclusion, the study shows that a linear relationship exists between force for delamination and the size of the indenter with a spherical nose. The relationship

is not affected by the presence of indentation damage. Therefore, finite element analysis that will be used to determine criteria for the delamination initiation need not include indentation damage in the models.

Acknowledgment

The work was sponsored by ISIS Canada and the Natural Science and Engineering Research Council of Canada (NSERC)—Research Grant Scheme. We are grateful to A. Yuen and B. Faulkner in the Department of Mechanical Engineering, University of Alberta for the technical assistance.

References

1. Standard Test Method for High Speed Puncture Properties of Plastics Using Load and Displacement Sensors, ASTM Standard D3763-02.
2. Standard Test Method for Measuring the Damage Resistance of a Fibr-Reinforced Polymer-Matrix Composite to a Concentrated Quasi-Static Indentation Force, ASTM Standard D 6264-98.
3. T. KUBOKI, P.-Y. B. JAR and J. J. R. CHENG, in preparation.
4. Protocols for Interlaminar Fracture Testing of Composites. European Structural Integrity Society (ESIS), Delft, The Netherlands, 1993.
5. M. DAVALLO, M. L. CLEMENS, H. TAYLOR and A. N. WILKINSON, *Plast. Rub. Compos. Proc. Appl.* **27** (1998) 384.

Received 28 January
and accepted 9 March 2004